Inorganic Chemistry
Article
Cite This: Inorg. Chem. XXXX, XXX, XXX−XXX
pubs.acs.org/IC

Palladium Nanoparticles Encapsulated in the MIL-101-Catalyzed One-Pot Reaction of Alcohol Oxidation and Aldimine Condensation

Yu-Yang Zhang,* Jia-Xin Li, Lin-Lin Ding, Lin Liu,* Shi-Ming Wang, and Zheng-Bo Han

College of Chemistry, Liaoning University, Shenyang 110036, P. R. China

Supporting Information

ABSTRACT: A bifunctional catalyst, Pd nanoparticles (NPs) encapsulated in MIL-101, has been synthesized by capillary impregnation. The as-prepared Pd@MIL-101 was characterized by powder X-ray diffraction, N_2 physisorption, X-ray photoelectron spectroscopy, transmission electron microscopy, and high-angle annular dark field scanning transmission electron microscopy, indicating that Pd NPs were highly dispersed in the pores of MIL-101 without deposition of the nanoparticles on the external surface or aggregation. The bifunctional catalyst of Pd@MIL-101 exhibited highly catalytic activity for alcohol oxidation and aldimine condensation one-pot reactions, where Pd NPs affords good oxidation activity and MIL-101 offers Lewis acidity. In particular, Pd@MIL-101 yielded an effective catalytic performance with toluene as the solvent, K_2CO_3 as the co-catalyst, and 353 K as the optimum reaction temperature for the one-pot reaction. After five cycles of reuse, Pd@MIL-101 still shows high catalytic performance. Above all, it is found that the enhanced catalytic performance was achieved via the synergistic cooperation of MIL-101 and Pd NPs.

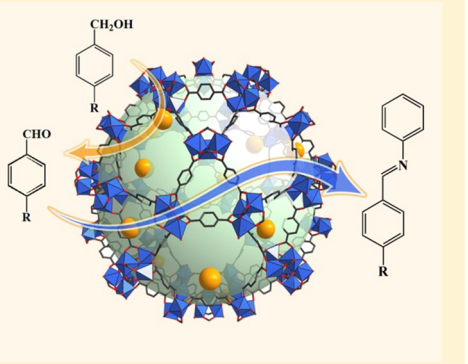

1. INTRODUCTION

Important factors in chemical engineering are solving the energy crisis and the problem of environmental pollution confronting the world. From a chemical synthesis point of view, the optimal solution is to combine two or more independent reactions into a cascade[1−5] or one pot.[6−11] When the reaction is performed in one pot, no intermediate separation or expensive purification is required, capital investment and manufacturing costs are reduced, and the economic competitiveness of the target compounds is improved. Alcohols,[12] a broad category of organic compounds, are of special interest as substrates for multistep organic reactions. For example, alcohols can be oxidized to aldehydes,[13] while further acetalization, alkylation,[14] or synthesis of imines affords their value-added products. The use of alcohol needs multistep catalytic processes. Therefore, the development of a one-pot heterogeneous system seems to be a promising option.

Metal−organic frameworks (MOFs),[15−18] a class of porous materials consisting of metal ions or clusters and organic ligands, have been widely investigated because of their uniform but tunable pores, large specific surface areas, diverse structures, and chemical durability.[19] MOFs have been utilized for many applications, including gas storage,[20] molecular sensing,[21] and catalysis.[22−28] For the past few years, MOFs have been extensively applied as heterogeneous catalysts,[29−32] especially those using MOFs as a carrier for metal nanoparticles.[33−37] Although a great deal of research has been done on the effect of MOFs in catalysis,[38−41] few studies have been conducted on metal@MOFs catalyzed for one-pot reactions. Huang et al. reported on the use of Pd/Cz-MOF-253−800 as a catalyst for a one-pot knoevenagel condensation−hydrogenation reaction.[42] Dong et al. developed the Cu414-MOF catalyst, a highly heterogeneous catalyst that promotes Friedel−Crafts alkylation of fluorene and acetals in a one-pot reaction at room temperature under solvent-free conditions.[43] Recently, Avelina et al. prepared a bifunctional MOF catalyst MOF-Cu(BTC)-[Pd], which is used in one-pot synthesis to achieve a series Sonogashira/click reaction.[33] As mentioned in the recent reviews, metal@MOFs for one-pot catalytic reactions still need to be studied further, especially the synergistic effect between the acidity and basicity of MOFs[42−44] and metal nanoparticles.[45] It has been reported that in a homogeneous system, Lewis acid/base and metal nanoparticles (NPs) can promote each other in combination due to a synergistic effect, thereby improving catalytic activity.[46] Inspired by some investigations,[33] we report here that Lewis acid and metal nanoparticles are combined to form metal NPs@Lewis acid MOFs to achieve a high-activity heterogeneous solid acid catalyst.

In this work, a bifunctional one-pot heterogeneous catalyst created by immobilization of Pd NPs in the cages of MIL-101 via an impregnation approach has been synthesized. The obtained Pd@MIL-101 catalyst combines the Pd NPs with the Lewis acid sites on MIL-101, which have successfully realized a one-pot reaction for selective oxidation of alcohols and then synthesis of imines. To the best of our knowledge, this is the

Received: August 4, 2018

DOI: 10.1021/acs.inorgchem.8b02206
Inorg. Chem. XXXX, XXX, XXX−XXX

first example that applies metal@MOF catalysts cooperatively in the one-pot alcohol oxidation and aldimine condensation reaction.

2. EXPERIMENTAL SECTION

2.1. Materials and Methods. All chemicals for synthesis were commercially available reagents of analytical grade and were used without further purification. The FT-IR spectra were recorded from KBr pellets in the range of 4000−400 cm^{-1} on a Nicolet 5DX spectrometer. Thermogravimetric analyses (TGA) were performed on a PerkinElmer Pyrisl instrument (25−800 °C, 5 °C min^{-1}, flowing N_2). Powder X-ray diffraction (powder XRD) was recorded with a Bruker AXS D8 advanced automated diffractometer with Cu Kα radiation. X-ray photoelectron spectroscopy (XPS) was performed on an ESCALAB 250Xi system equipped with Al Kα radiation. Transmission electron microscopy (TEM) was conducted on a JEOL-2010 electron microscope with an electron acceleration energy of 200 kV. The high-angle annular dark field scanning transmission electron microscopy (HAADF-STEM) images were recorded on a JEM-2100F electron microscope operated at 200 kV. Energy-dispersive X-ray (EDX) spectra were collected with a field emission instrument of the type SU8010. Gas sorption isotherms were performed with a Belsorp-Max automatic volumetric adsorption apparatus. The sample was soaked with dimethylformamide (DMF) for 24 h. After the removal of DMF by decanting, the sample was soaked in anhydrous ethanol for 24 h and then dried under dynamic vacuum (<10^{-3} Torr) at 423 K overnight. Before the measurement, the sample was dried again by using the "outgas" function of the surface area analyzer for 4 h at 423 K. The content of Pd in Pd@MIL-101 was quantified by inductively coupled plasma atomic emission spectroscopy (ICP-AES). The catalytic reaction products were analyzed and identified with an SP-2100A gas chromatograph (equipped with a Kromat-Bond Series capillary column and a flame ionization detector).

2.2. Synthesis of the Catalyst. *2.2.1. Synthesis of MIL-101.* MIL-101 was synthesized by the previously reported hydrothermal method[47] with a slight modification. Because HF is harmful to the environment, acetic acid (99.5%) was chosen to replace it. Briefly, $Cr(NO_3)_3{\cdot}9H_2O$ (3.20 g, 8.00 mmol), H_2BDC (1.31 g, 7.88 mmol), and acetic acid (2.17 mL, 0.038 mmol) were added to 40 mL of ultrapure water. This mixture was sonicated at room temperature and placed in an 80 mL Teflon reactor, and the reactor was sealed, placed in an oven, and kept at 473 K for 8 h. The fine green suspensions were collected and washed three times with DMF and ethanol, respectively, using centrifugation (10000 rpm for 15 min) and sonication. Finally, the MIL-101 particles were evacuated in a vacuum oven at 423 K for 12 h to obtain dehydrated products prior to further use.

2.2.2. Synthesis of Pd@MIL-101. In this paper, Pd@MIL-101 catalysts with different Pd NPs loadings were prepared via a simple capillary impregnation−reduction method.[48] First, 50 mg of activated MIL-101 (the volume of pore is 1.5 cm^3/g) was placed in the vials, to which 80 μL of Na_2PdCl_4 (0.17 mol/L, 0.01 mmol) methanol was added dropwise. More importantly, the solution volume of Na_2PdCl_4 was smaller than the pore volume of MIL-101, so that the solution of Na_2PdCl_4 could be absorbed into the pores of MIL-101 completely. Then, ∼3 mL of a 0.6 mol/L $NaBH_4$ methanol solution was added dropwise while the mixture was being stirred until the color of the solution became dark. The as-prepared samples were designated as 2.0%-Pd@MIL-101, where 2.0% represents the Pd NPs loading. After filtration, the synthesized sample was further placed under dynamic vacuum at 423 K for 12 h to obtain dehydrated Pd@MIL-101. A similar method was applied for preparation of 1.0%-Pd@MIL-101 and 4.0%-Pd@MIL-101 nanocomposites by adjusting the concentration of Na_2PdCl_4 in methanol; the concentrations of Na_2PdCl_4 in the two catalysts were 0.085 and 0.34 mol/L.

2.3. Evaluation of Catalytic Activity. *2.3.1. Alcohol Oxidation.* The oxidation reaction was performed in a three-neck flask equipped with a condenser. Alcohol (1 mmol), catalyst *x*%-Pd@MIL-101 (1 mmol %), and co-catalyst (0.7 mmol) were added to 4 mL of solvent. During the reaction, the mixture was vigorously stirred and pumped with oxygen through a long needle (1 atm, 5 mL/min). The reaction samples were monitored by gas chromatography (GC).[49]

2.3.2. Alcohol Oxidation and Aldimine Condensation One-Pot Reaction. The alcohol oxidation−aldimine condensation reaction was also performed in a three-neck flask equipped with a condenser. After alcohol oxidation was finished, aniline (1.5 mmol) was added to the mixture at a constant temperature of 353 K for 1 h. Prior to GC analysis, the catalyst in the reaction system was separated by centrifugation. When the process was finished, the catalyst was washed with methanol and dried under vacuum for reuse.

2.3.3. Leaching Test. The catalyst 2.0%-Pd@MIL-101 was separated from the solution right after the reaction for 2 h, and the reaction was continued in the absence of the catalyst for an additional 2 h.

3. RESULTS AND DISCUSSION

3.1. Characterization of the Catalysts. The as-prepared MIL-101 matches well with the simulated pattern reported by Férey et al.,[50] revealing that MIL-101 has been successfully synthesized. The powder XRD patterns (Figure 1) and IR

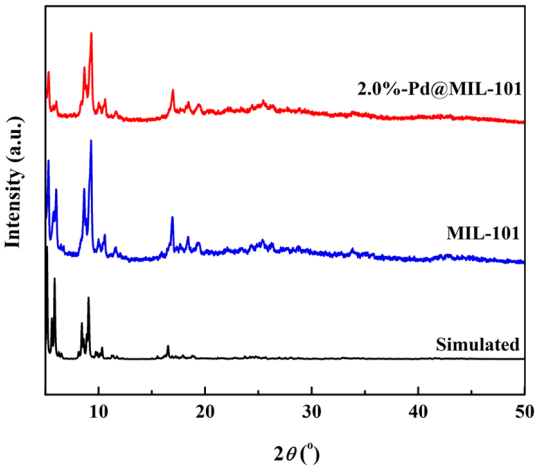

Figure 1. Powder XRD patterns of simulated MIL-101, as-prepared MIL-101, and 2.0%-Pd@MIL-101.

spectra (Figure S1) of Pd@MIL-101 confirm that the structure of the MIL-101 maintained its crystalline integrity during the loading process. No diffractions are detected for Pd NPs from PXRD patterns after $NaBH_4$ reduction in Pd@MIL-101 with different Pd loadings, indicating that Pd loadings are too low or Pd NPs are too small in all samples, which is similar to the results reported by Jiang et al.[45] The loading amount of Pd was 1.01, 2.00, and 4.05 wt % determined by ICP-AES. According to the TG results (Figure S2), we can conclude that Pd@MIL-101 exhibits high thermal stability below 673 K, which is similar to that of MIL-101.

The specific surface areas and pore volumes of the catalyst are the important parameters. Because the loading of the Pd NPs can affect the surface area and pore volume, the surface area and the pore volume of Pd@MIL-101 with different Pd loadings were determined by N_2 physisorption measurements at 77 K (Figure 2a). The BET surface area and the total pore volume of bare MIL-101 are 2869 $m^2\ g^{-1}$ and 1.50 $m^3\ g^{-1}$, respectively, which are consistent with previous reports.[51] The isotherms have two uptake steps around P/P_0 values of 0.1 and 0.2, revealing there are two kinds of pores in the crystal structure. The pore size distribution curve exhibits two different pore sizes of 2.4 and 3.0 nm (Figure 2b), which are

DOI: 10.1021/acs.inorgchem.8b02206
Inorg. Chem. XXXX, XXX, XXX−XXX

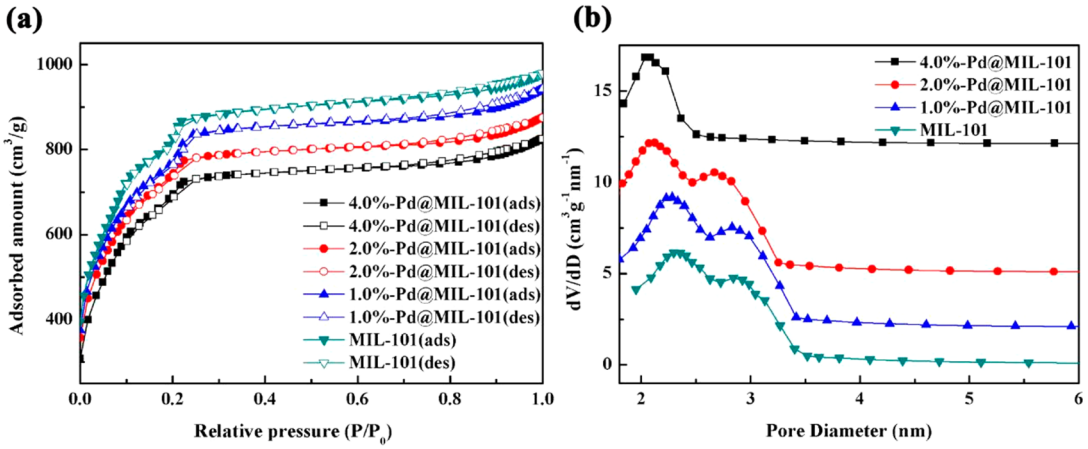

Figure 2. (a) N_2 adsorption isotherms at 77 K of as-synthesized MIL-101 and Pd@MIL-101. (b) Pore size distribution of as-synthesized MIL-101 and *x*%-Pd@MIL-101 samples.

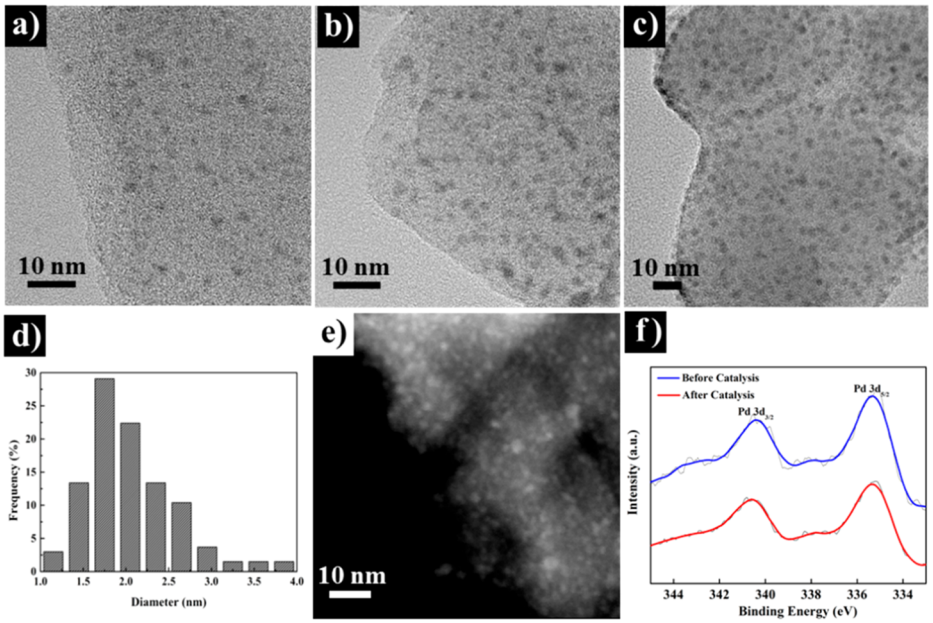

Figure 3. TEM images of as-prepared products with various Pd loadings: (a) 1.0%-Pd@MIL-101, (b) 2.0%-Pd@MIL-101, and (c) 4.0%-Pd@MIL-101. (d) Pd NP particle size distribution histogram of 2.0%-Pd@MIL-101. (e) HAADF-STEM image showing the ultrafine Pd NPs in 2.0%-@MIL-101. (f) XPS spectra of Pd 3d for 2.0%-Pd@MIL-101 before and after catalysis.

close to the reported values of Hupp et al.[52] Compared with those of MIL-101, the BET surface areas and total pore volumes of all of the *x*%-Pd@MIL-101 species are decreased. For 1.0%-Pd@MIL-101, the BET surface area and total pote volume are 2740 $m^2\ g^{-1}$ and 1.50 $cm^3\ g^{-1}$, respectively. For 2.0%-Pd@MIL-101 and 4.0%-Pd@MIL-101, the BET surface area and total pore volume are decreased to 2612 $m^2\ g^{-1}$ and 1.31 $cm^3\ g^{-1}$ and 2546 $m^2\ g^{-1}$ and 1.13 $cm^3\ g^{-1}$, respectively, mainly because of the highly dispersed Pd NPs occupying the cavities of MIL-101. At the same time, the pore sizes of *x* %-Pd@MIL-101 are slightly decreased because of the incorporation of Pd NPs (Figure 2b).

TEM images of *x*%-Pd@MIL-101 are shown in Figure 3a–c. The loading amount and size of the Pd NPs are affected the concentration of Na_2PdCl_4. As the concentration of Na_2PdCl_4 increased, the amounts and particle sizes of Pd NPs clearly increased. For 2.0%-Pd@MIL-101, most Pd NPs with a narrow particle size distribution of 1.8 ± 1 nm were formed within the pores of MIL-101 without deposition of the Pd NPs on the external surface or aggregation (Figure 3b,d). Moreover, the HAADF-STEM image was taken, and the results demonstrated that Pd NPs were trapped inside MIL-101 (Figure 3e). The pore sizes of MIL-101 are 2.4 and 3.0 nm, and the Pd NPs in 2.0%-Pd@MIL-101 can be held in the pores, leaving some space for the diffusion of the reactant. EDX spectra of 2.0%-Pd@MIL-101 are shown in Figure S3, where the Pd element is present with the Cr element, indicating Pd was effectively captured by MIL-101. The XPS results show that Pd NPs are in reduced states (Figure 3f). However, the particle size of the Pd NPs is 2.5 ± 1 nm of 4.0%-Pd@MIL-101, which is larger than the MIL-101 pore sizes. Therefore, the pores of the MIL-101 are partly blocked by the Pd nanoparticles. At the same time, some of the particles also aggregated on the surface of MIL-101.

3.2. Evaluation of Catalytic Activity. *3.2.1. Exploration of Alcohol Oxidation Reaction Conditions.* Our first catalytic

DOI: 10.1021/acs.inorgchem.8b02206
Inorg. Chem. XXXX, XXX, XXX–XXX

objective was to investigate whether the Pd NPs in MIL-101 would perform well as catalysts. We first investigated their activity in the synthesis of benzaldehyde via the alcohol oxidation reaction. To evaluate the catalytic performance and optimize the reaction conditions, we explored the effects of the type of solvents, reaction temperature, catalyst dosage, reaction time, and inorganic base on the alcohol oxidation reaction. MIL-101 and Pd/C were employed as the comparison. Table 1

Table 1. Alcohol Oxidation Reaction with Different Solvents, Inorganic Bases, and Temperatures in the Presence of the Pd@MIL-101 Catalyst[a]

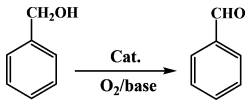

entry	catalyst (mol %)	solvent	T (K)	inorganic base	t (h)	yield[b] (%)
1	1.0%-Pd@MIL-101 (1.0)	toluene	353	K_2CO_3	4	76.7
2	2.0%-Pd@MIL-101 (1.0)	toluene	353	K_2CO_3	4	99.9
3	4.0%-Pd@MIL-101 (1.0)	toluene	353	K_2CO_3	4	84.8
4	2.0%-Pd@MIL-101 (0.5)	toluene	353	K_2CO_3	4	89.9
5	2.0%-Pd@MIL-101 (1.5)	toluene	353	K_2CO_3	4	>99.9
6	2.0%-Pd@MIL-101 (1.0)	1,4-dioxane	353	K_2CO_3	4	12.0
7	2.0%-Pd@MIL-101 (1.0)	DMSO	353	K_2CO_3	4	18.1
8	2.0%-Pd@MIL-101 (1.0)	DMF	353	K_2CO_3	4	36.0
9	2.0%-Pd@MIL-101 (1.0)	*o*-xylene	353	K_2CO_3	4	91.4
10	2.0%-Pd@MIL-101 (1.0)	toluene	353	Na_2CO_3	4	75.0
11	2.0%-Pd@MIL-101 (1.0)	toluene	353	KOH	4	84.6
12	2.0%-Pd@MIL-101 (1.0)	toluene	333	K_2CO_3	4	46.2
13	2.0%-Pd@MIL-101 (1.0)	toluene	343	K_2CO_3	4	78.3
14	2.0%-Pd@MIL-101 (1.0)	toluene	353	K_2CO_3	1	39.2
15	2.0%-Pd@MIL-101 (1.0)	toluene	353	K_2CO_3	2	59.3
16	2.0%-Pd@MIL-101 (1.0)	toluene	353	K_2CO_3	3	79.1
17	2.0%-Pd@MIL-101 (1.0)	toluene	353	none	4	67.1
18[c]	Pd/C	toluene	353	K_2CO_3	4	55.4
19[d]	MIL-101	toluene	353	K_2CO_3	–	–
20[e]	none	toluene	353	none	4	<1

[a]Reaction conditions: alcohol (1 mmol), base (0.7 mmol), solvent (4 mL), O_2 (0.1 MPa). [b]Yield determined by GC analysis. [c]Using 0.4 mol % commercial 5% Pd/C. [d]Using 0.01 mmol of MIL-101. [e]No catalyst.

shows the generation of benzaldehyde at 353 K in the presence of Pd@MIL-101 with different Pd loadings and K_2CO_3 as a binary catalyst. For 1.0 mol % 1.0%-Pd@MIL-101, 2.0%-Pd@MIL-101, and 4.0%-Pd@MIL-101 (Table 1, entries 1−3, respectively), benzaldehyde was obtained in good yields (76.7−99.9%). Among them, catalyst 2.0%-Pd@MIL-101 can serve as an excellent catalyst for the synthesis of benzaldehyde with a highest yield of 99.9% (Table 1, entry 2). A different amount of the 2.0%-Pd@MIL-101 catalyst was also used to confirm the influence of the amount of Pd on the reaction. As shown in entries 2, 4, and 5 of Table 1, when the amount of 2.0%-Pd@MIL-101 decreases to 0.5 mol % the yield of the benzaldehyde also decreases to 89.9%. Therefore, for 1.0%-Pd@MIL-101, the Pd content is too small, so the yield is reduced. For 4.0%-Pd@MIL-101, because many Pd particles aggregated in the hole of the MOF, the yield dropped. A total of 1.0 mol % catalyst afforded a satisfying yield, so this catalyst loading amount was fixed for the following experiments.

Then, we investigated the influence of organic solvents on the catalytic system. The catalytic reactions were performed in 1,4-dioxane, dimethyl sulfoxide (DMSO), DMF, *o*-xylene, and toluene. It was evident that toluene is a suitable solvent for the alcohol oxidation reaction, while 1,4-dioxane, DMSO, DMF, and *o*-xylene afforded lower yields (Table 1, entries 6−9). As the polarity of the solvent increased, the conversion of the reactants increased. It may be that the polarity of aromatic solvents is more similar to that of aromatic alcohols, and they have better solubility and are beneficial to the aerobic oxidation of aromatic alcohols. It is noteworthy that the yield decreased to 75.0 and 84.6% when the base was changed to Na_2CO_3 and KOH (Table 1, entries 10 and 11, respectively), respectively, indicating that K_2CO_3 was a superior base for this reaction. Furthermore, the reaction temperature and reaction time greatly affected the reaction rates. The results showed that the rate increased when the temperature increased from 333 to 353 K (Table 1, entries 2, 12, and 13) and the reaction time increased from 1 to 4 h (Table 1, entries 2 and 14−16), indicating that the optimal reaction temperature and reaction time were 353 K and 4 h, respectively. We also tested 5% Pd/C as a control catalyst. The yield for benzaldehyde was 64.9% under the same reaction condition (Table 1, entry 18), while the yield for benzaldehyde was very poor when bare MIL-101 or K_2CO_3 was used without Pd NPs in the reaction system, under the employed conditions (Table 1, entries 17 and 19). Moreover, it was found that the catalytic reaction almost did not occur when both Pd@MIL-101 and K_2CO_3 were absent (Table 1, entry 20).

3.2.2. Oxidation Reaction of Various Alcohols. After optimizing the reaction conditions, we attempted to extend the catalytic system to oxidation of a series of alcohols using a 2.0%-Pd@MIL-101 catalyst (Table 2). It can be seen that 2.0%-Pd@MIL-101 was highly active and selective for the oxidation of most of the substrates, indicating the high versatility of the MOF-supported catalyst. It is interesting to note that the aromatic alcohols containing electron-donating groups (-OCH_3, -CH_3, and -H) gave obviously yields (96.2−99.9%, Table 2, entries 1−3, respectively) that were higher than those containing electron-withdrawing groups (-NO_2 and -Cl) (64.3−66.6%, Table 2, entries 4 and 5, respectively), indicating that the electronic effect of the reactant also affects the yields in using Pd@MIL-101 as a catalyst. However, these benzylic alcohols were converted to the corresponding aldehydes with high selectivity. In addition, we explored our methodology for the oxidization of cinnamon alcohol and 3-phenylpropanol, which have similar structures. However, the conversion rates are quite different in the same 12 h. It is obvious that aromatic alcohols with conjugated structures are also easy to oxidize and have high selectivity (Table 2, entries 6 and 7). Many reviews have reported that aliphatic alcohols are difficult to oxidize;[52,53] however, in this study, cyclohexane and

DOI: 10.1021/acs.inorgchem.8b02206
Inorg. Chem. XXXX, XXX, XXX−XXX

Table 2. Catalytic Oxidation of Alcohols Using 2.0%-Pd@MIL-101[d]

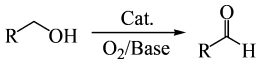

Entry	Substrates	Product	t (h)	Conv.[c](%)	Select.[c] (%)
1[a]	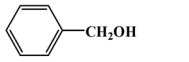	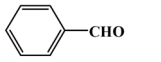	8	96.2	100
2[a]	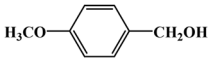	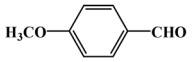	4	99.9	100
3[a]	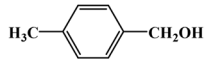	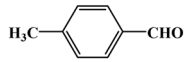	8	99.9	100
4[a]	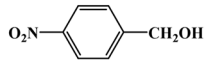	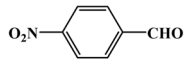	12	64.3	100
5[a]	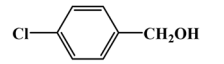	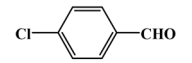	12	66.6	100
6[a]	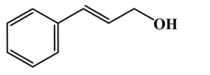	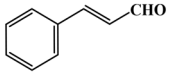	12	99.9	100
7[a]	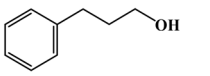	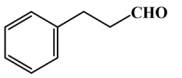	12	25	83
8[a]	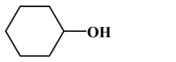	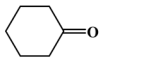	12	15	61
9[a]	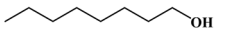		12	10	50
10[b]	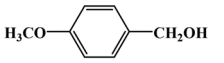	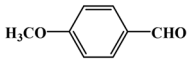	12	trace	-

[a]In 2.0%-Pd@MIL-101 (1.0 mol %). [b]No 2.0%-Pd@MIL-101. [c]Determined by GC. [d]Reaction conditions: alcohol (1 mmol), K_2CO_3 (0.7 mmol), toluene (4 mL), O_2 (0.1 MPa), 353 K.

octanol[54] have been transformed to the corresponding aldehydes under extremely mild reaction conditions, and the selectivity is considerable (Table 2, entries 8 and 9). To test the necessity of 2.0%-Pd@MIL-101, we conducted a control experiment using only 4-methoxybenzyl alcohol and a co-catalyst and found that the substrate showed little conversion (Table 2, entry 10). In conclusion, 2.0%-Pd@MIL-101 is an excellent catalyst for oxidation of both aromatic alcohols and aliphatic alcohols with high efficiency and high selectivity.

3.2.3. Bifunctional Catalysis. It is widely accepted that imines make up a very necessary class of intermediates in the synthesis of all kinds of pharmaceutical, agricultural, and biological compounds. Many types of organic reactions such as reduction, addition, condensation, cycloaddition, and multi-component reactions are used for the synthesis of imine.[55,56] A conventional method for the synthesis of imines is reaction of aldehydes or ketones with amines under certain conditions.[57,58] In this experiment, imines were synthesized directly from the one-pot reaction of alcohols and amines, catalyzed by multifunctional catalyst Pd@MIL-101, which did not require the separation of the segregating product aldehydes or ketones during the alcohol oxidation reaction.

As shown in Table 3, 2.0%-Pd@MIL-101 was an active catalyst for this one-pot reaction and 99.0% conversion of 4-methoxybenzyl alcohol with 99.9% selectivity to target production of *N*-(4-methoxybenzylidene)aniline was achieved in 4.8 h (Table 3, entry 1). A series of control experiments were performed to investigate the function of 2.0%-Pd@MIL-101 in the one-pot reaction. MIL-101 gave only trace conversion of 4-methoxybenzyl alcohol (Table 3, entry 4), which confirmed the oxidation of 4-methoxybenzyl alcohol to

Table 3. One-Pot Oxidation−Condensation Reaction Catalyzed by 2.0%-Pd@MIL-101[a]

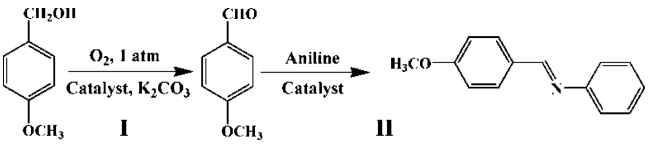

				yield[c] (%)	
entry	reaction[a]	catalyst[b]	*t* (h)	b	c
1	one-pot (I + II)	2.0%-Pd@MIL-101	4.8	trace	99.9
2	one-pot (I + II)	MIL-101	5	trace	–
3	one-pot (I + II)	none	5	–	–
4	I	MIL-101	4	trace	–
5	I	2.0%-Pd@MIL-101	4	99.9	–
6	I	Pd/C	4	64.9	–
7	I	none	4	trace	–
8	II	MIL-101	1	–	99.9
9	II	Pd/C	1	–	43.1
10	II	2.0%-Pd@MIL-101	0.8	–	99.9
11	II	none	1	–	40.5

[a]Reaction conditions: (I) alcohol (1 mmol), K_2CO_3 (0.7 mmol), 2%-Pd@MIL-101 (1.0 mol %), toluene (4 mL), O_2 (0.1 MPa), 353 K; (II) aniline (1.5 mmol). [b]Using 0.01 mmol of MIL-101. [c]Determined by GC.

DOI: 10.1021/acs.inorgchem.8b02206
Inorg. Chem. XXXX, XXX, XXX−XXX

4-methoxybenzaldehyde is catalyzed by Pd NPs. For comparison, a commercial Pd/C as a control catalyst was measured under the same conditions, while a 64.9% yield of *N*-(4-methoxybenzylidene)aniline was achieved (Table 3, entry 6). This can further verify that 2.0%-Pd@MIL-101 possesses superior activity for the oxidation reaction compared to that of the commercial Pd/C catalyst. To confirm that the condensation reaction is catalyzed by MIL-101, we tested the activity of MIL-101 in the condensation reaction using 4-methoxybenzaldehyde and aniline as the substrates. It was found that MIL-101 achieved a 99.9% yield after 1 h in the aldehyde condensation reaction (Table 3, entry 8), which verified that MIL-101 is a highly active catalyst in the condensation reaction. These catalysis results show that both Pd NPs and Lewis acid sites on MIL-101 are essential for the one-pot oxidation−condensation reaction and the high activity mainly due to the highly dispersed Pd NPs confinement effect in cages of MIL-101. Therefore, 2.0%-Pd@MIL-101 is a highly efficient multifunctional catalyst.

On the basis of the aforementioned experiments and previous reports,[59] the mechanism for the alcohol oxidation−aldimine condensation reaction can be proposed to be the noble metal and Lewis acid-based catalysis tentatively. There are two kinds of active sites in Pd@MIL-101. For the alcohol oxidation reaction, first, a Pd atom inserts into the O−H bond of the alcohol to form a metal alkoxide and a metal hydride. Then, through a β-hydride elimination process, the desired product aldehyde is produced by removing a hydrogen from the Pd alkoxide. At the same time, the Pd-based catalyst absorbs a hydrogen molecule. Finally, the active site of the Pd-based catalyst is regenerated through the oxidation of adsorbed hydrogen by oxygen (Figure S4). For the aldimine condensation reaction, the Lewis active site is the Cr(III). First, the carbonyl group in the aldehyde coordinates with Cr(III), which enhances the electrophilicity of the aldehyde carbonyl group. Then, the arylamine is subjected to a nucleophilic addition reaction to obtain an α-amino alcohol, which is further heated and dehydrated to obtain an imine product and regenerate the acitve sites of Cr(III) (Figure S5).

3.3. Leaching Experiment. The reaction profile for the reaction of 4-methoxybenzyl alcohol and O_2 over 2.0%-Pd@MIL-101 is shown in Figure S6a. The yield of the oxidation reaction using 2.0%-Pd@MIL-101 as a catalyst gradually increased from 0 to 4 h. To demonstrate that no Pd NPs were dissolved in the solvent during the oxidation reaction, the 2.0%-Pd@MIL-101 catalyst was removed after 2 h (Figure S6b). The reaction no longer proceeded when the catalyst was removed. This was consistent with ICP-AES analysis as Pd traces (0.25 mg L^{-1}) were observed in the reaction solution. Therefore, during the oxidation reaction, there were no Pd NPs leaching into the solvent, and MIL-101 as a support perfectly protected the loading Pd NPs. It can be seen from Figure 3f that there was no change in the valence state of Pd after the reaction.

3.4. Recycling Experiment. The reusability of 2.0%-Pd@MIL-101 was examined. After an initial reaction, the solid catalyst was isolated from the liquid phase by centrifugation and then reused in additional runs. The 2.0%-Pd@MIL-101 catalyst could be recycled at least five times (Figure S7). This proved that the multifunctional catalyst Pd@MIL-101 had advantages of recycling.

After the reaction, we recovered the catalysts by centrifugal separation. XRD data of 2.0%-Pd@MIL-101 before and after the reaction are shown in Figure S8. A low-angle diffraction peak was observed for the 2.0%-Pd@MIL-101 curve before and after the reaction, indicating that the framework structure was stable during the reaction. TEM observations (Figure S9) further demonstrated that the size and distribution of Pd NPs remained almost unchanged after five reactions. According to the ICP-AES results, significant Pd leaching during the reaction was also excluded here, wherein the concentration of Pd species leached in the reaction solution was 0.25 mg L^{-1}. They all verified Pd@MIL-101 was a highly reliable multifunctional catalyst.

4. CONCLUSIONS

A multifunctional heterogeneous one-pot catalyst Pd@MIL-101 for alcohol oxidation and aldimine condensation has been developed. The as-prepared Pd@MIL-101 catalyst exhibits high efficiency and selectivity for the alcohol oxidation−aldimine condensation reaction because of the special pore structure, Pd NPs, and the existence of Lewis acidity on MIL-101, and there are no Pd NPs leaching into the system during the reaction cycle experiment that showed that Pd@MIL-101 can be reused five times without any loss of activity or selectivity, showing good potential for practical application. All of the experimental results adequately show MIL-101 is a very suitable supporter and Pd@MIL-101 has commendable stability. Meanwhile, it more fully illustrates that MOFs are superb supports and catalysts. Further work on exploring more multifunctional MOFs as heterogeneous catalysts to catalyze more significant one-pot reactions is expected.

■ ASSOCIATED CONTENT

Supporting Information

The Supporting Information is available free of charge on the ACS Publications website at DOI: 10.1021/acs.inorgchem.8b02206.

Supplementary physical characterizations and catalysis (PDF)

■ AUTHOR INFORMATION

Corresponding Authors

*E-mail: yyzhang@lnu.edu.cn.

*E-mail: liulin@lnu.edu.cn.

ORCID

Lin Liu: 0000-0002-9164-1190

Zheng-Bo Han: 0000-0001-8635-9783

Notes

The authors declare no competing financial interest.

■ ACKNOWLEDGMENTS

This work was financially supported by the National Natural Science Foundation of China (Grants 21701076, 21671090, and 21501084). The authors gratefully thank the Collaborative Innovation Group of Clean Energy Resources for kind help in catalyst characterization.

■ REFERENCES

(1) Perez-Gomez, M.; Hernandez-Ponte, S.; Bautista, D.; Garcia-Lopez, J. A. Synthesis of Spiro-Oxoindoles through Pd-Catalyzed Remote C-H Alkylation Using Alpha-Diazocarbonyl Compounds. *Chem. Commun.* **2017**, *53*, 2842−2845.

(2) Baylon, R. A. L.; Sun, J.; Kovarik, L.; Engelhard, M.; Li, H.; Winkelman, A. D.; Wang, Y. Structural Identification of $Zn_xZr_yO_z$

DOI: 10.1021/acs.inorgchem.8b02206
Inorg. Chem. XXXX, XXX, XXX−XXX

Catalysts for Cascade Aldolization and Self-Deoxygenation Reactions. *Appl. Catal., B* **2018**, *234*, 337−346.
(3) Chen, L.; Yan, J.; Tong, Z.; Yu, S.; Tang, J.; Ou, B.; Yue, L.; Tian, L. Nanofiber-Like Mesoporous Alumina Supported Palladium Nanoparticles as a Highly Active Catalyst for Base-Free Oxidation of Benzyl Alcohol. *Microporous Mesoporous Mater.* **2018**, *266*, 126−131.
(4) Strange, E. F.; Hill, J. M.; Coetzee, J. A. Evidence for a New Regime Shift between Floating and Submerged Invasive Plant Dominance in South Africa. *Hydrobiologia* **2018**, *817*, 349−362.
(5) Ding, Y.-L.; Li, S.-N.; Cheng, Y. Selective Synthesis of Multifunctionalized 2,3-Dihydroinden-1-ones and 1,3-Dihydroisobenzofurans from the Reaction of o-Alkynylbenzaldehydes with Imines Steered by N-Heterocyclic Carbene/Copper(II) and N-Heterocyclic Carbene/Base Cascade Catalysis. *J. Org. Chem.* **2018**, *83*, 8971.
(6) Xi, J.; Sun, H.; Wang, D.; Zhang, Z.; Duan, X.; Xiao, J.; Xiao, F.; Liu, L.; Wang, S. Confined-Interface-Directed Synthesis of Palladium Single-Atom Catalysts on Graphene/Amorphous Carbon. *Appl. Catal., B* **2018**, *225*, 291−297.
(7) Liu, J.-G.; Chen, W.-W.; Gu, C.-X.; Xu, B.; Xu, M.-H. Access to Spiroindolines and Spirodihydrobenzofurans via Pd-Catalyzed Domino Heck Spiroyclization through C−H Activation and Carbene Insertion. *Org. Lett.* **2018**, *20*, 2728−2732.
(8) Wang, Y.-T.; Fang, Z.; Yang, X.-X.; Yang, Y.-T.; Luo, J.; Xu, K.; Bao, G.-R. One-Step Production of Biodiesel from *Jatropha* Oils with High Acid Value at Low Temperature by Magnetic Acid-Base Amphoteric Nanoparticles. *Chem. Eng. J.* **2018**, *348*, 929−939.
(9) Tian, X.; Zhou, M.; Tan, C.; Li, M.; Liang, L.; Li, K.; Su, P. KOH Activated N-Doped Novel Carbon Aerogel as Efficient Metal-Free Oxygen Reduction Catalyst for Microbial Fuel Cells. *Chem. Eng. J.* **2018**, *348*, 775−785.
(10) Zhang, Y.; Wang, Y.-X.; Liu, L.; Wei, N.; Gao, M.-L.; Zhao, D.; Han, Z.-B. Robust Bifunctional Lanthanide Cluster Based Metal−Organic Frameworks (MOFs) for Tandem Deacetalization−Knoevenagel Reaction. *Inorg. Chem.* **2018**, *57*, 2193−2198.
(11) Lee, W.-P.; Kong, X.-Y.; Tan, L.-L.; Gui, M.-M.; Sumathi, S.; Chai, S.-P. Molybdenum Disulfide Quantum Dots Decorated Bismuth Sulfide as a Superior Noble-Metal-Free Photocatalyst for Hydrogen Evolution through Harnessing a Broad Solar Spectrum. *Appl. Catal., B* **2018**, *232*, 117−123.
(12) Date, N. S.; Chikate, R. C.; Roh, H.-S.; Rode, C.-V. Bifunctional Role of Pd/MMT-K 10 Catalyst in Direct Transformation of Furfural to 1,2-Pentanediol. *Catal. Today* **2018**, *309*, 195−201.
(13) Anand, M.; Farooqui, S.-A.; Singh, J.; Singh, H.; Sinha, A. K. Mechanistic in-Operando FT-IR Studies for Hydroprocessing of Triglycerides. *Catal. Today* **2018**, *309*, 11−17.
(14) Slavík, P.; Lhoták, P. Unusual Reactivity of Upper-Rim Bridged Calix[4]Arenes−Friedel−Crafts alkylation via cleavage of the macrocyclic skeleton. *Tetrahedron Lett.* **2018**, *59*, 1757−1759.
(15) Gong, X.; Wang, W.-W.; Fu, X.-P.; Wei, S.; Yu, W.-Z.; Liu, B.; Jia, C.-J.; Zhang, J. Metal-Organic-Framework Derived Controllable Synthesis of Mesoporous Copper-Cerium Oxide Composite Catalysts for the Preferential Oxidation of Carbon Monoxide. *Fuel* **2018**, *229*, 217−226.
(16) Han, Y.; Yu, Y.; Zhang, L.; Huang, L.; Zhai, J.; Dong, S. Facile Synthesis of Ni based Metal-Organic Frameworks Wrapped MnO_2 Nanowires with High Performance toward Electrochemical Oxygen Evolution Reaction. *Talanta* **2018**, *186*, 154−161.
(17) Majhi, S. M.; Naik, G. K.; Lee, H.-J.; Song, H.-G.; Lee, C.-R.; Lee, I.-H.; Yu, Y.-T. Au@NiO Core-Shell Nanoparticles as a p-Type Gas Sensor: Novel Synthesis, Characterization, and Their Gas Sensing Properties with Sensing Mechanism. *Sens. Actuators, B* **2018**, *268*, 223−231.
(18) Liu, Y.; Luo, R.; Li, Y.; Qi, J.; Wang, C.; Li, J.; Sun, X.; Wang, L. Sandwich-Like Co_3O_4/MXene Composite with Enhanced Catalytic Performance for Bisphenol A degradation. *Chem. Eng. J.* **2018**, *347*, 731−740.
(19) Zhang, W.; Wu, W.; Long, Y.; Wang, F.; Ma, J. Co-Ag Alloy Protected by Nitrogen doped Carbon as Highly Efficient and Chemoselective Catalysts for the Hydrogenation of Halogenated Nitrobenzenes. *J. Colloid Interface Sci.* **2018**, *522*, 217−227.
(20) Betard, A.; Fischer, R.-A. Metal-Organic Framework Thin Films: from Fundamentals to Applications. *Chem. Rev.* **2012**, *112*, 1055−83.
(21) Kreno, L.-E.; Leong, K.; Farha, O.-K.; Allendorf, M.; Van Duyne, R.-P.; Hupp, J.-T. Metal-Organic Framework Materials as Chemical Sensors. *Chem. Rev.* **2012**, *112*, 1105−25.
(22) Zhang, H.; Liu, X.; Wu, Y.; Guan, C.; Cheetham, A.-K.; Wang, J. MOF-Derived Nanohybrids for Electrocatalysis and Energy Storage: Current Status and Perspectives. *Chem. Commun.* **2018**, *54*, 5268−5288.
(23) Liu, P.-P.; Zhu, H.-L.; Zheng, Y.-Q. Hybrid MnO/C Nanorod Arrays Derived from a MOF Precursor with Enhanced Oxygen Evolution Activity. *J. Mater. Sci.* **2018**, *53*, 11574−11583.
(24) Gong, Y.; Zhao, X.; Zhang, H.; Yang, B.; Xiao, K.; Guo, T.; Zhang, J.; Shao, H.; Wang, Y.; Yu, G. MOF-Derived Nittogen Doped Carbon Modified g-C_3N_4 Heterostructure Composite with Enhanced Photocatalytic Activity for Bisphenol Adegradation with Peroxymonosulfate under Visible Light Irradiation. *Appl. Catal., B* **2018**, *233*, 35−45.
(25) Liu, J.; Hao, J.; Hu, C.; He, B.; Xi, J.; Xiao, J.; Wang, S.; Bai, Z. Palladium Nanoparticles Anchored on Amine-Functionalized Silica Nanotubes as a Highly Effective Catalyst. *J. Phys. Chem. C* **2018**, *122*, 2696−2703.
(26) Duan, X.; Liu, J.; Hao, J.; Wu, L.; He, B.; Qiu, Y.; Zhang, J.; He, Z.; Xi, J.; Wang, S. Magnetically Recyclable Nanocatalyst with Synergetic Catalytic Effect and Its Application for 4-Nitrophenol Reduction and Suzuki Coupling Reactions. *Carbon* **2018**, *130*, 806−813.
(27) Duan, X.; Xiao, M.; Liang, S.; Zhang, Z.; Zeng, Y.; Xi, J.; Wang, S. Ultrafine Palladium Nanoparticles Supported on Nitrogen-Doped Carbon Microtubes as a High-Performance Organocatalyst. *Carbon* **2017**, *119*, 326−331.
(28) Xi, J.; Xiao, J.; Xiao, F.; Jin, Y.; Dong, Y.; Jing, F.; Wang, S. Mussel-Inspired Functionalization of Cotton for Nano-Catalyst Support and Its Application in a Fixed-Bed System with High Performance. *Sci. Rep.* **2016**, *6*, 21904.
(29) Bakuru, V.-R.; Velaga, B.; Peela, N.-R.; Kalidindi, S.-B. Hybridization of Pd Nanoparticles with UiO-66(Hf) Metal-Organic Framework and the Effect of Nanostructure on the Catalytic Properties. *Chem. - Eur. J.* **2018**, DOI: 10.1002/chem.201803200.
(30) Hermes, S.; Schroter, M.-K.; Schmid, R.; Khodeir, L.; Muhler, M.; Tissler, A.; Fischer, R.-W.; Fischer, R.-A. Metal@MOF: Loading of Highly Porous Coordination Polymers Host Lattices by Metal Organic Chemical Vapor Deposition. *Angew. Chem., Int. Ed.* **2005**, *44*, 6237−41.
(31) Zanon, A.; Verpoort, F. Metals@ZIFs: Catalytic Applications and Size Selective Catalysis. *Coord. Chem. Rev.* **2017**, *353*, 201−222.
(32) Xu, Z.; Zhang, W.; Weng, J.; Huang, W.; Tian, D.; Huo, F. Encapsulation of Metal Layers within Metal−Organic Frameworks as Hybrid Thin Films for Selective Catalysis. *Nano Res.* **2016**, *9*, 158−164.
(33) Arnanz, A.; Pintado-Sierra, M.; Corma, A.; Iglesias, M.; Sánchez, F. Bifunctional Metal Organic Framework Catalysts for Multistep Reactions: MOF-Cu(BTC)-[Pd] Catalyst for One-Pot Heteroannulation of Acetylenic Compounds. *Adv. Synth. Catal.* **2012**, *354*, 1347.
(34) Aijaz, A.; Karkamkar, A.; Choi, Y.-J.; Tsumori, N.; Rönnebro, E.; Autrey, T.; Shioyama, H.; Xu, Q. Immobilizing Highly Catalytically Active Pt Nanoparticles inside the Pores of Metal−Organic Framework: A Double Solvents Approach. *J. Am. Chem. Soc.* **2012**, *134*, 13926−13929.
(35) Jiang, H.-L.; Akita, T.; Ishida, T.; Haruta, M.; Xu, Q. Synergistic Catalysis of Au@Ag Core-Shell Nanoparticles Stabilized on Metal-Organic Framework. *J. Am. Chem. Soc.* **2011**, *133*, 1304−6.
(36) Li, X.; Zhang, B.; Fang, Y.; Sun, W.; Qi, Z.; Pei, Y.; Qi, S.; Yuan, P.; Luan, X.; Goh, T.-W.; Huang, W. Metal-Organic-Framework-Derived Carbons: Applications as Solid-Base Catalyst and Support for

DOI: 10.1021/acs.inorgchem.8b02206
Inorg. Chem. XXXX, XXX, XXX−XXX

Pd Nanoparticles in Tandem Catalysis. *Chem. - Eur. J.* **2017**, *23*, 4266−4270.
(37) Zhu, N.-X.; Zhao, C.-W.; Wang, J.-C.; Li, Y.-A.; Dong, Y.-B. Micro-Cu4I4-MOF: Reversible Iodine Adsorption and Catalytic Properties for Tandem Reaction of Friedel-Crafts Alkylation of Indoles with Acetals. *Chem. Commun.* **2016**, *52*, 12702−12705.
(38) Yang, Q.; Xu, Q.; Jiang, H.-L. Metal-Organic Frameworks Meet Metal Nanoparticles: Synergistic Effect for Enhanced Catalysis. *Chem. Soc. Rev.* **2017**, *46*, 4774−4808.
(39) Xiao, J.-D.; Han, L.; Luo, J.; Yu, S.-H.; Jiang, H.-L. Integration of Plasmonic Effects and Schottky Junctions into Metal-Organic Framework Composites: Steering Charge Flow for Enhanced Visible-Light Photocatalysis. *Angew. Chem., Int. Ed.* **2018**, *57*, 1103−1107.
(40) Chen, Y.-Z.; Wang, Z.-U.; Wang, H.; Lu, J.; Yu, S.-H.; Jiang, H.-L. Singlet Oxygen-Engaged Selective Photo-Oxidation over Pt Nanocrystals/Porphyrinic MOF: The Roles of Photothermal Effect and Pt Electronic State. *J. Am. Chem. Soc.* **2017**, *139*, 2035−2044.
(41) Liu, H.; Xu, C.; Li, D.; Jiang, H.-L. Photocatalytic Hydrogen Production Coupled with Selective Benzylamine Oxidation over MOF Composites. *Angew. Chem., Int. Ed.* **2018**, *57*, 5379−5383.
(42) Li, H.; Yang, T.; Fang, Z. Biomass-Derived Mesoporous Hf-Containing Hybrid for Efficient Meerwein-Ponndorf-Verley Reduction at Low Temperatures. *Appl. Catal., B* **2018**, *227*, 79−89.
(43) Sun, P.; Wang, W.; Weng, X.; Dai, X.; Wu, Z. Alkali Potassium Induced HCl/CO_2 Selectivity Enhancement and Chlorination Reaction Inhibition for Catalytic Oxidation of Chloroaromatics. *Environ. Sci. Technol.* **2018**, *52*, 6438−6447.
(44) Chung, Y.-M. One-pot Cascade Deacetalization and Nitroaldol Condensation over Acid−Base Bifunctional ZIF-8 Catalyst. *Res. Chem. Intermed.* **2018**, *44*, 3673−3685.
(45) Gu, X.; Lu, Z.-H.; Jiang, H.-L.; Akita, T.; Xu, Q. Synergistic Catalysis of Metal-Organic Framework-Immobilized Au-Pd Nanoparticles in Dehydrogenation of Formic Acid for Chemical Hydrogen Storage. *J. Am. Chem. Soc.* **2011**, *133*, 11822−5.
(46) Yamamoto, H.; Futatsugi, K. "Designer Acids": Combined Acid Catalysis for Asymmetric Synthesis. *Angew. Chem., Int. Ed.* **2005**, *44*, 1924−42.
(47) Chen, G.; Wu, S.; Liu, H.; Jiang, H.; Li, Y. Palladium Supported on an Acidic Metal−Organic Framework as an Efficient Catalyst in Selective Aerobic Oxidation of Alcohols. *Green Chem.* **2013**, *15*, 230−235.
(48) Yadav, M.; Xu, Q. Catalytic Chromium Reduction Using Formic Acid and Metal Nanoparticles Immobilized in a Metal-Organic Framework. *Chem. Commun.* **2013**, *49*, 3327−9.
(49) Zhou, Z.; He, C.; Xiu, J.; Yang, L.; Duan, C. Metal-Organic Polymers Containing Discrete Single-Walled Nanotube as a Heterogeneous Catalyst for the Cycloaddition of Carbon Dioxide to Epoxides. *J. Am. Chem. Soc.* **2015**, *137*, 15066−9.
(50) Ferey, G. Hybrid Porous Solids: Past, Present, Future. *Chem. Soc. Rev.* **2008**, *37*, 191−214.
(51) Chen, Y.; Guo, Z.; Chen, T.; Yang, Y. Surface-Functionalized TUD-1 Mesoporous Molecular Sieve Supported Palladium for Solvent-Free Aerobic Oxidation of Benzyl Alcohol. *J. Catal.* **2010**, *275*, 11−24.
(52) Nguyen, H.-G.; Weston, M.-H.; Farha, O.-K.; Hupp, J.-T.; Nguyen, S.-T. A Catalytically Active Vanadyl(Catecholate)-Decorated Metal Organic Framework via Post-Synthesis Modifications. *CrystEngComm* **2012**, *14*, 4115.
(53) Su, F.-Z.; Liu, Y.-M.; Wang, L.-C.; Cao, Y.; He, H.-Y.; Fan, K.-N. Ga−Al Mixed-Oxide-Supported Gold Nanoparticles with Enhanced Activity for Aerobic Alcohol Oxidation. *Angew. Chem.* **2008**, *120*, 340−343.
(54) Liu, H.; Liu, Y.; Li, Y.; Tang, Z.; Jiang, H. Metal−Organic Framework Supported Gold Nanoparticles as a Highly Active Heterogeneous Catalyst for Aerobic Oxidation of Alcohols. *J. Phys. Chem. C* **2010**, *114*, 13362−13369.
(55) Kobayashi, S.; Ishitani, H. Catalytic Enantioselective Addition to Imines. *Chem. Rev.* **1999**, *99*, 1069−1094.
(56) Ma, J. A. Catalytic Asymmetric Synthesis of Alpha- and Beta-Amino Phosphonic Acid Derivatives. *Chem. Soc. Rev.* **2006**, *35*, 630−636.
(57) Patil, R.-D.; Adimurthy, S. Catalytic Methods for Imine Synthesis. *Asian J. Org. Chem.* **2013**, *2*, 726−744.
(58) Largeron, M.; Fleury, M.-B. Bioinspired Oxidation Catalysts. *Science* **2013**, *339*, 43−44.
(59) Guo, Z.; Liu, B.; Zhang, Q.; Deng, W.; Wang, Y.; Yang, Y. Recent Advances in Heterogeneous Selective Oxidation Catalysis for Sustainable Chemistry. *Chem. Soc. Rev.* **2014**, *43*, 3480−524.

DOI: 10.1021/acs.inorgchem.8b02206
Inorg. Chem. XXXX, XXX, XXX−XXX